

Improving the performance of bilayer aluminum-rubber composite plate under high energy rate impact; numerical and experimental investigation

Abstract

This paper aims to investigate the performance of an aluminum–rubber composite plate under a high-speed impact condition. The impact resistance of the plate has been evaluated using both experimental and numerical methods. The experimental test was carried out using a high-speed gas gun at velocities of 144 m/s and 168 m/s. The energy absorption and failure mechanisms of composite plate has been closely examined for all samples. The effect of the rubber layer positioning either on front face or on back face of the aluminum plate was also evaluated. It was found that the composite plate with rubber on front face provides higher performance to absorb the energy. In parallel to the experiment, a finite element computer model was created using commercial software to simulate the response of the aluminum–rubber composite plate under a high energy rate loading condition. The data obtained from finite element modeling shown a close agreement with the experimental results in terms of failure mechanism and energy absorption. In addition, a parametric study was carried out incorporating different impact velocities, rubber formulation, rubber layer thickness and interface bonding strength between the rubber and aluminum layer. It was concluded that by increasing the rubber layer’s thickness the energy absorption of the composite plate will be increased, especially when rubber layer placed in front face of the aluminum plate. Although at high interface bonding of rubber and aluminum layers, the composite with rubber layer in front face has better performance, but low bonding of interface lead to higher energy absorption in back face configuration.

Keywords: High velocity impact, Aluminum-rubber composite, Energy absorption, LS-DYNA.

1. Introduction

Structural protection against high impact projectiles using aluminum alloy has been a topic of interest for many years due to its low weight, reasonable formability and high impact strength. The topic was the interest of many researches and a considerable number of scientific papers focusing on the dynamic response, impact resistance, and failure of aluminum alloys has been published using experimental and numerical methods [1-4]. The ultimate target of these researches were to find an improved alloy of aluminum to be replaced with the traditional steel alloys.

In recent years, researchers have made a significant efforts to improve the performance of metallic structural protections against high impact threats [ref?]. One major development has been the use of elastomeric coatings on hard substrates to decrease the damages of blast load and penetration of projectiles. Elastomers have been widely used to dissipate kinetic energy associated with impacts and shocks. Multilayer elastomers have been shown promising results in these applications. Polyurea is a elastomer which can be used as a layer and create a metal-elastomer composite structure. Amini et al. [5, 6] investigated the response of monolithic steel plates and steel-polyurea bilayer plates subjected to impulsive and direct pressure pulse. The research was carried out experimentally and numerically, focusing on the deformation and failure modes of the plates. Their results suggested that the polyurea layer can have a significant effect on the response of the steel plate onto dynamic impulsive loads. They have considered the failure mitigation and energy absorption of the plate, if the layer attached on

the back face of the plate. Roland et al. [7, 8] reported the ability of polyurea coatings to increase the impact resistance of high hardness steel plates, where they observed the effect of different layer configurations on the residual velocity. They showed that when polyurea applied to the strike face of steel plates provides a significant enhancement in the ballistic resistance of these plates. They have concluded that the most possible reason for this improvement against impact resistance of the polyurea-coated steel is a phase transition of the polyurea from the rubbery phase to the glassy phase. This hypothesis was supported by Grujicic [9] using a computational model to evaluate the energy absorption when a deformation-induced glass transition occurs.

Natural rubber (NR) is an appropriate material which can be used as a layer on a rigid substrate. Rubber materials have been widely used in shock absorbers, impact resistance panels and other engineering applications [10]. High level of damping property [11], high level of flexibility [12], and excellent puncture and tear resistance [13] are the specific properties of NR. These features make NR a good candidate to be used as a reinforcement in a composite structure [14-16]. To convert a raw NR into a material with desired properties, some ingredients such as fillers, activators, sulfur or other equivalent curatives and accelerators should be added to the raw NR. Variation of compound ingredients alters the mechanical properties of rubber [17]. These additives modify the rubber by forming cross-links between polymer chains. One of the most important ingredients, is filler including carbon black and calcium carbonate [18-20]. These fillers are added to rubber formulation to improve the mechanical properties of NR.

The main objective of this research is analysis of failure and energy absorption of an aluminum-rubber composite plate perforated by a projectile. Perforation tests were conducted

using hemispherical projectiles with impact velocities of 144 m/s and 168 m/s. During the experiments, the focus was on the significance of positioning the rubber layer onto the front face or onto the back face of the aluminum plate. The intention was to find out which position provides more energy absorption. In parallel, the failure mode of layer was closely monitored and the observation was mimicked to create a computer simulation. The numerical model was then used to carry a series of parametric studies. The model was also used to investigate the parameters which affect the impact resistance of a bilayer aluminum-rubber composite plate.

2. Experimental procedure

2.1. Materials and specimen preparation

Aluminum alloy has been used as a candidate material in many engineering applications due to its low density and high ductility and its reasonable strength. In this study, Aluminum 2024 was used for the experimental tests. The mechanical specification of Aluminum 2024 which was obtained from a tensile testing, is given in Table 1.

Table 1 Mechanical properties of aluminum 2024

Property	Value
Density, ρ (kg/m ³)	2700
Elastic modulus, E (MPa)	72200
Yield stress, σ_y (MPa)	350
Poisson ratio, ν	0.32

Natural rubber (SMR 20) with Mooney viscosity of 65 was used as the other layered material in this study. The SMR 20 material was supplied by the Rubber Research Institute of Malaysia. Compound ingredients named fillers such as carbon black and calcium carbonate were added to the rubber formulation to improve its mechanical properties. In the rubber compound, ZnO, stearic acid, accelerators and sulfur constitute the vulcanization system

which is used for crosslinking of the matrix phase. To evaluate the behavior of rubber with different components at high strain rates, two types of rubber with different formulation were used. The two types of compounds with a high hardness (HH) and a low hardness (LH) are presented in Table 2. Compounding were performed on an open two-roll mixing mill (Polymix 200 L, Germany) and were cured under hydraulic pressure according to the rheometer results which is presented in Fig.1 for both LH and HH rubber.

Table 2 Formulation of the rubber compounds

Ingredients	Loading (Phr)	
	Formulation 1	Formulation 2
NR	100	100
Carbon Black (N330)	60	40
Zink oxide	5	5
Calcium carbonate	30	30
Spindle oil	15	30
Sulfur	2	1.5
Volcacit	0.7	0.7

To prepare the specimens, a layer of aluminum and rubber were bonded together by BYLAMET S2 adhesive. Before bonding, the aluminum plate were cleaned with acetone. To obtain a strong bonding between aluminum and rubber plates, a pressure was applied on the specimen. The pressure-time relation was concluded base on Fig 1 graph.

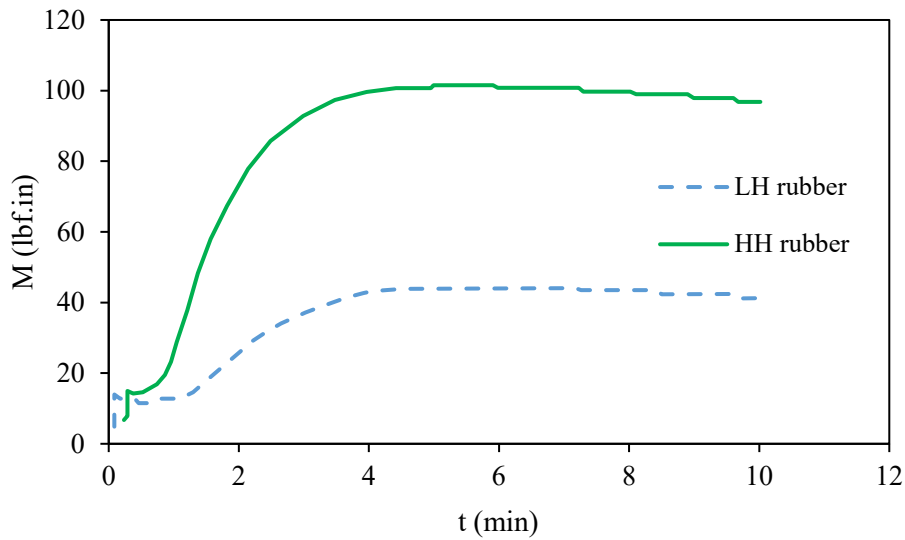


Fig. 1 Rheometer curves

2.2. High velocity impact tests

High velocity impact tests were performed using a gas gun shown in Fig.2. The gas gun is made of a pressure vessel with a 120 bar capacity, a high speed firing valve and a hollow steel barrel of 6 m long. The inside diameter of the barrel is 10 mm. The exact impact velocity of each projectile was measured with a chronograph (model M-1, Chrony Canada) immediately before and after impacting the target. Fixtures for holding the specimens were located in the target chamber. The projectile used for ballistic tests was made of steel and had a hemispherical cylindrical shape with a diameter of 10 mm and mass of 9.32 g. The projectiles were hardened by heat treatment to minimize projectiles' deformation.

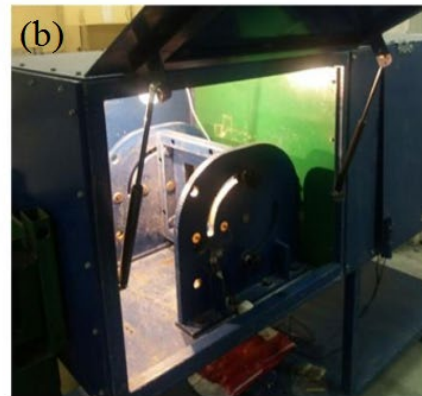


Fig. 2 (a) Gas gun (b) Target chamber

2.3. SHPB experiment

High strain rate tests on the rubber sample were conducted using Split Hopkinson Pressure Bar (SHPB) to obtain the samples stress–strain properties at different strain rates. The conventional steel SHPB helps to test metallic materials, but it cannot precisely determine the dynamic responses of soft materials like rubber [21]. The tests were performed using nylon bars instead of metal bar owing to this limitation. The mechanical impedance of nylon bars is much closer to that of the rubber specimens. Thus, the transmitted wave is sufficiently large for measurement. The Split Hopkinson Pressure Bar (SHPB) system, striker bar and rubber specimen are presented in Fig. 3. The ratio of optimal length-to-diameter (L/D) in the specimens for the SHPB test is 0.5, which was used to minimize inertia and friction effects [22]. To ensure homogeneous deformation and stress equilibrium during the experiment, the length of soft material specimens must be sufficiently short. In this study, the length of the specimen was designed to be 5 mm.

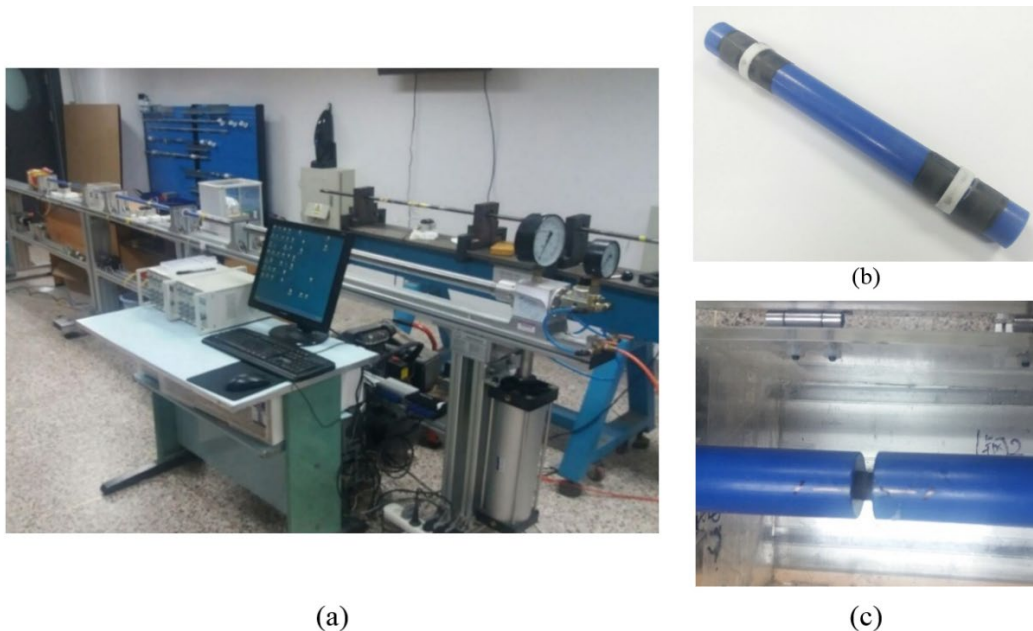


Fig. 3 Split Hopkinson Pressure Bar test (a) SHPB machine (b) Striker bar (c) rubber Specimen.

3. Numerical analysis

The commercial finite element software, LS-DYNA V9.71, was used for impact simulation. LS-DYNA is a non-linear dynamic modeling software that benefits explicit formulation and was used to simulate the response of rubber panel under high velocity impact. Projectile diameter, sample constraints and dimension were set according to those used in the experiment.

3.1. Material modeling

3.1.1. Aluminum plate

Material model 3 in LS-DYNA software (MAT_PLASTIC_KINEMATIC) was chosen to describe the elastic–plastic behavior of the aluminum plate. This material model uses an isotropic constitutive based on isotropic and kinematic hardening [23]. Also, strain rate effects are estimated by Cowper–Symonds constitutive relationship.

$$\sigma_{y-dyn} = [1 + (\frac{\dot{\epsilon}}{C})^{\frac{1}{P}}] (\sigma_{y-st} + E_P \epsilon_P) \quad (1)$$

In Eq. (1), P and C are empirical constants, and for aluminum alloys are 4 and 6500 1/s, respectively [24, 25].

3.1.2. Rubber layer

LS-DYNA offers several material models for simulation of rubber-like materials. In this research Mooney-Rivlin model was chosen with the strain energy function given by:

$$W = C_{10} (I_1 - 3) + C_{01} (I_2 - 3) \quad (2)$$

where I_1 and I_2 are the principal invariants of the left Cauchy–Green deformation tensor, defined by:

$$\begin{aligned}
I_1 &= \text{tr } \mathbf{C} = \lambda_1^2 + \lambda_2^2 + \lambda_3^2 \\
I_2 &= \frac{1}{2} [(\text{tr } \mathbf{C})^2 - \text{tr } \mathbf{C}^2] = \lambda_1^2 \lambda_2^2 + \lambda_1^2 \lambda_3^2 + \lambda_2^2 \lambda_3^2 \\
I_3 &= \det \mathbf{C} = \lambda_1 \lambda_2 \lambda_3
\end{aligned} \tag{3}$$

λ_1 , λ_2 and λ_3 are the principal stretches. The Mooney–Rivlin model does not take the strain rate effect into consideration. However, with certain adjustment, the Mooney–Rivlin model can be used in the simulations. Figs. 4 shows the stress–strain curves at different strain rates obtained by SHPB tests for both LH and HH natural rubbers. The strain rate that the material undergoes during the penetration process was estimated by impact simulation on a pure rubber panel. The study applied a strain rate about 4000 s^{-1} for the rubber and fitted it with Mooney–Rivlin material model, using the least squares approach. The calibrated coefficients of C_{10} and C_{01} are 5.6 and 0.5, respectively for the high hardness rubber and 2.9 and 0.4 for the low hardness rubber. The maximum principal strain is used as the failure criterion of the rubbers. The entire rubber panel was modeled by LS-DYNA and impact response of the panel was simulated and verified by a pervious experimental work [26]. Although, results of quasi-static test show the HH and LH rubber elongation to break are about 220 % and 350% under quasi-static test, but from a series of simulations, it was estimated that the failure elongation for the rubber material is 120% and 170% under high strain rates.

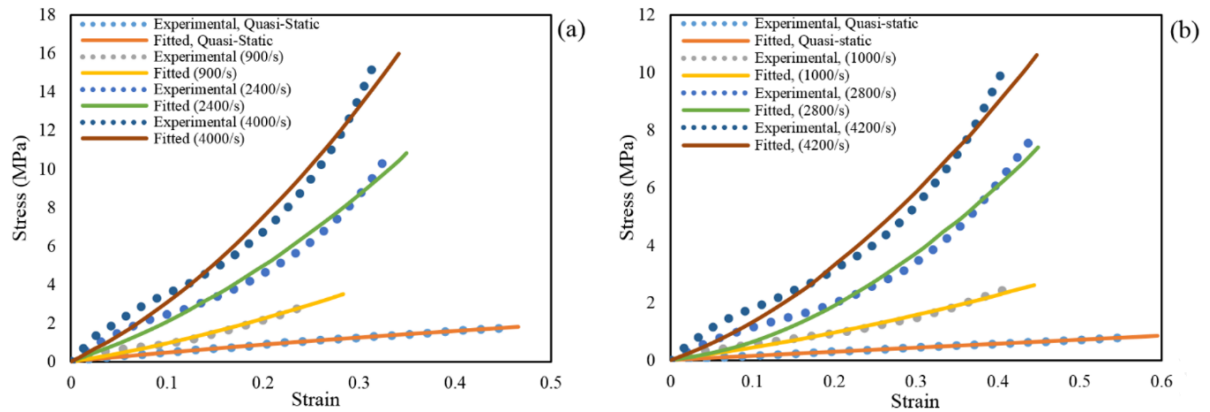


Fig. 4 Stress-Strain curves of rubber at different strain rates (a) high hardness rubber (b) low hardness rubber

4. Results and discussion

The main objective of this study is to investigate the behavior and impact resistance of the combined two-layer aluminum-rubber composite plate, including the energy absorption and failure mechanism of the composite plate. A series of experimental tests and numerical analyses were performed on single layered aluminum plate and double layer aluminum-rubber samples.

4.1. Impact on aluminum plate

To evaluate the impact resistance of aluminum plate, impact tests were conducted using gas gun at four different velocities of 96, 109, 122 and 129 m/s. The hemispherical projectile impacted the 0.5 mm aluminum plate, and the residual velocities, global deformations and the fracture mechanisms were evaluated. For such a thick plate, the failure mechanics was petaling, with four petals characteristically. By increasing the impact velocity, larger petals were shown at penetration zone.

A numerical simulation was performed to investigate the high velocity impact on the aluminum plate. This was done in parallel with the experiment to validate the energy absorption of the target plate at velocities which experiments were performed. The failure

mode also was compared with the experiments. Fig. 5 shows the perforated aluminum plate at incidence velocity of 109 m/s. Four petals formed at this velocity has been compared experimentally and numerically in Fig. 5a-b. The compared results show that the simulated numerical model is in close agreement with the experiment.. The simulated penetration process is shown in Fig. 6.

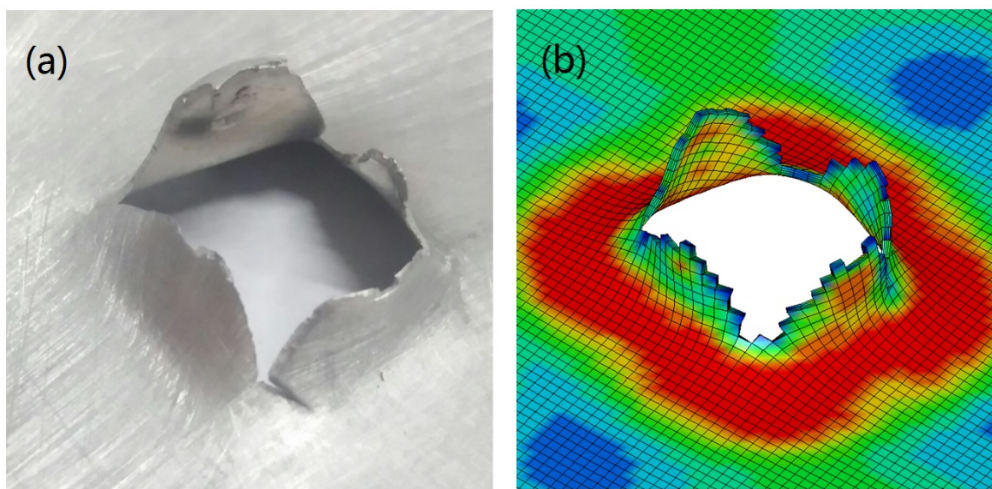


Fig 5 Comparison of (a) experimental and (b) numerical results at initial velocity of 109 m/s.

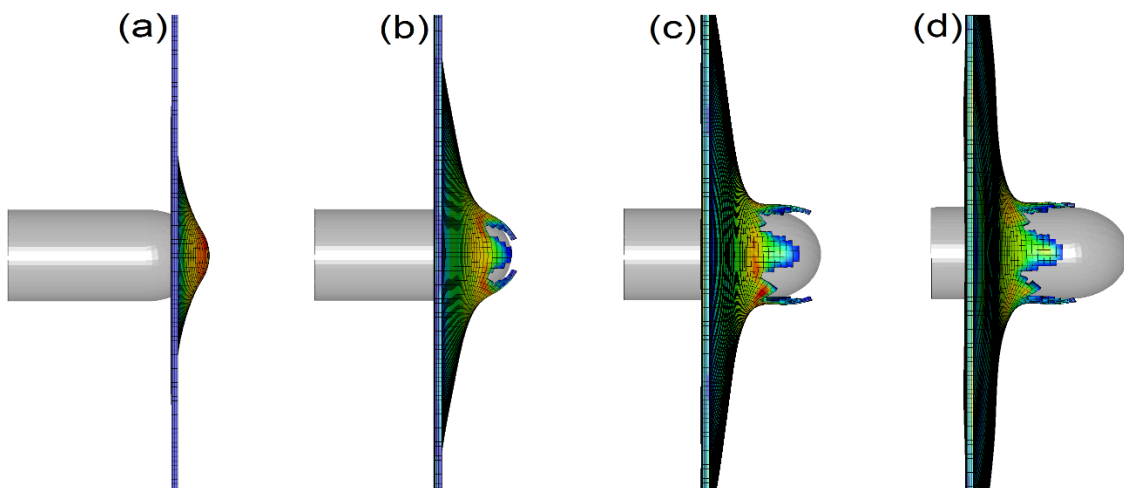


Fig 6 Perforation of projectile at initial velocity of 129 m/s at (a) 30 (b) 60 (c) 90 and (d) 120 μ s time interval.

The projectile's residual velocity versus the impact initial velocity is shown in Fig. 7. Simulations show a good agreement with the experimental test results. To define the threshold for the penetration velocity, a simulation was carried out in which the residual velocity become zero. The reference velocity was found to be 50.5 m/s.

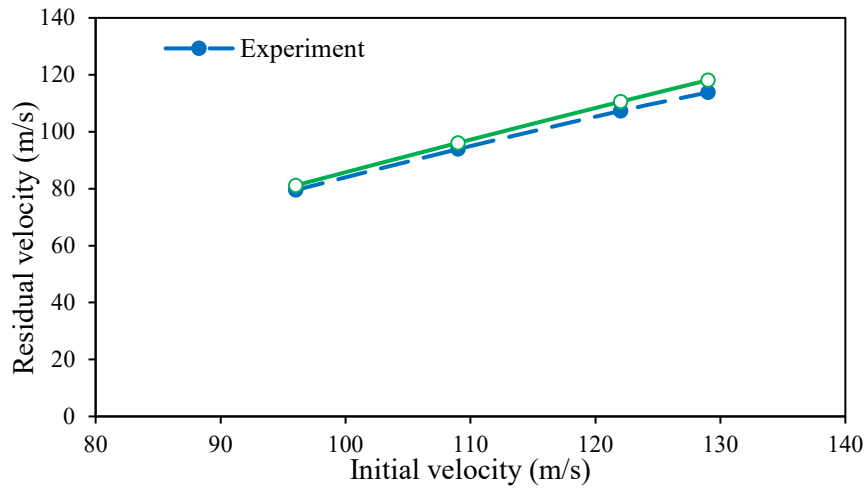


Fig 7 Experimental and numerical comparison of residual velocity versus impact velocity after perforating the aluminum plate

4.2. Impact on aluminum-rubber plate

The aluminum-rubber bilayer samples were setup using two different configurations: the rubber on the impact face (front face; FF) and on the face opposite to the impact side (back face; BF).

Tests were conducted at two different velocities of 144 m/s and 168 m/s. Each speed was repeated five times and the average velocity was calculated for each test group.

To model the experimentally observed debonding of the aluminum and rubber layers, a FE model was created considering the aluminum and rubber layers. Contact algorithm option of CONTACT_AUTOMATIC_SURFACE_TO_SURFACE_TIEBREAK which is embedded in

LS-DYNA software, was used to define the contact between the rubber and aluminum plate. The velocities were set to those already used in the experiment.

In the FE model, it was assumed that the interface debonding is governed by the following failure criterion:

$$\left(\frac{\sigma}{NFLS}\right)^2 + \left(\frac{\tau}{SFLS}\right)^2 \geq 1 \quad (4)$$

Where σ and τ are the normal and shear stresses at the interface, and SFLS and NFLS are the interface normal and shearing strengths. Because there was no experimental data on the bonding strength at the time, a trial and error method was employed to reproduce the experimentally observed debonding by adjusting the value of the interface bonding strength. The bonding strength was numerically predicted as 80 MPa for SFLS and 50 MPa for NFLS. Mechanical behavior of the composite plate obtained experimentally and numerically for the two FF and Bf configurations as shown in Figs. 8 and 9. It can be observed that the estimated data for bonding strength values can be used to predict reasonably the debonding of composite layers under impact loading.

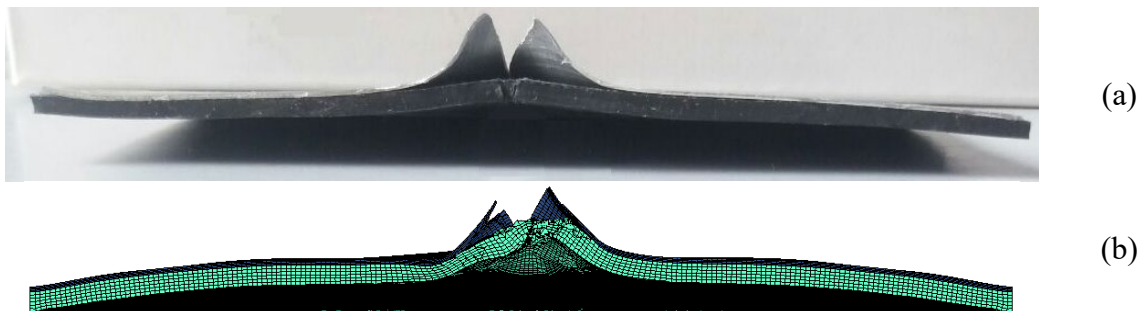


Fig 8 Comparison of (a) experimental and (b) numerical results with the rubber on the front face at the impact velocity of 144 m/s



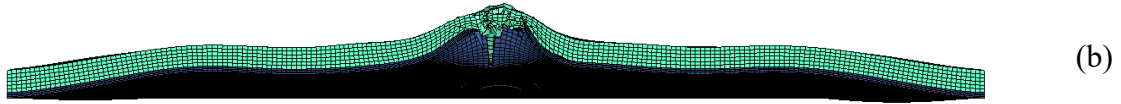


Fig 9 Comparison of (a) experimental and (b) numerical results with the rubber on the back face at the impact velocity of 144 m/s

The experimental and numerical behavior of the aluminum-rubber composite plate under impact loading are presented in Figs. 10-13. Figures 10 and 11 shows the response of the composite plate when the rubber layer located on the back face (BF) under the impact velocity of 144 m/s and 168 m/s, respectively. Also, response of the composite plate when the rubber layer is located on the front face (FF) under the similar impact velocities is shown in Figs. 12 and 13. A good agreement is shown for both configurations comparing numerical and experimental results.

From principal of energy absorption, the ballistic performance of a composite can be calculated. It was assumed that the loss of projectile's kinetic energy is equal to the energy absorption performed by the composite target in at the perforation event. Therefore the energy absorption of the composite target can be theoretically calculated by subtracting the residual energy of the projectile from its initial energy as presented below.

$$E_p = \frac{1}{2} m_p (V_i^2 - V_r^2) \quad (5)$$

Where E_p (J) is dissipated energy during the impact process, m_p (kg) is the mass of the projectile, V_i (m/s) is the initial velocity of the projectile, and V_r (m/s) the residual velocity. Table 3 presents the experimental and numerical results performed for BF and FF configurations. In this table, experimental test results performed at velocities of 144 and 168 are presented. A high hardness rubber layer was used. The residual velocity of the projectile was measured after perforating the aluminum-rubber composite, and the energy absorption

was determined using Equation (5). Energy absorption was used as a criteria to evaluate the ballistic performance of the composite plate. The experimental result was used to validate the numerical simulation. Table 3 indicates that the numerical model can be used to estimate the projectile residual velocity and the energy absorption by the bi-layer composite. The maximum error in this numerical model is less than 10%.

Table 3 Comparison of energy absorption obtained by experimental and numerical simulation

Configuration	Impact velocity (m/s)	Experimental residual velocity (m/s)	Numerical residual velocity (m/s)	Experimental energy absorption (J)	Numerical energy absorption (J)	Error (%)
Rubber in back face	144	114.6	117.2	35.4	32.6	7.9
	168	138.7	141.5	41.9	38.2	8.8
Rubber in front face	144	104.5	107	45.7	43.3	5.2
	168	133.9	137.6	48	43.3	9.8

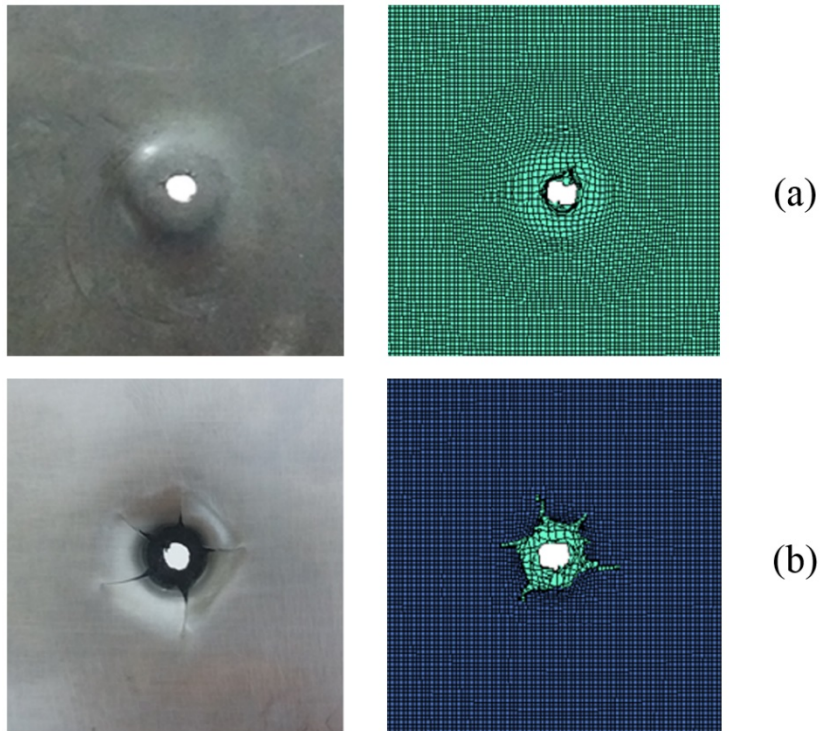


Fig 10 Failure of composite with the rubber on the back face at the impact velocity of 144 m/s obtained Experimentally and numerically (a) Back view (b) Front view

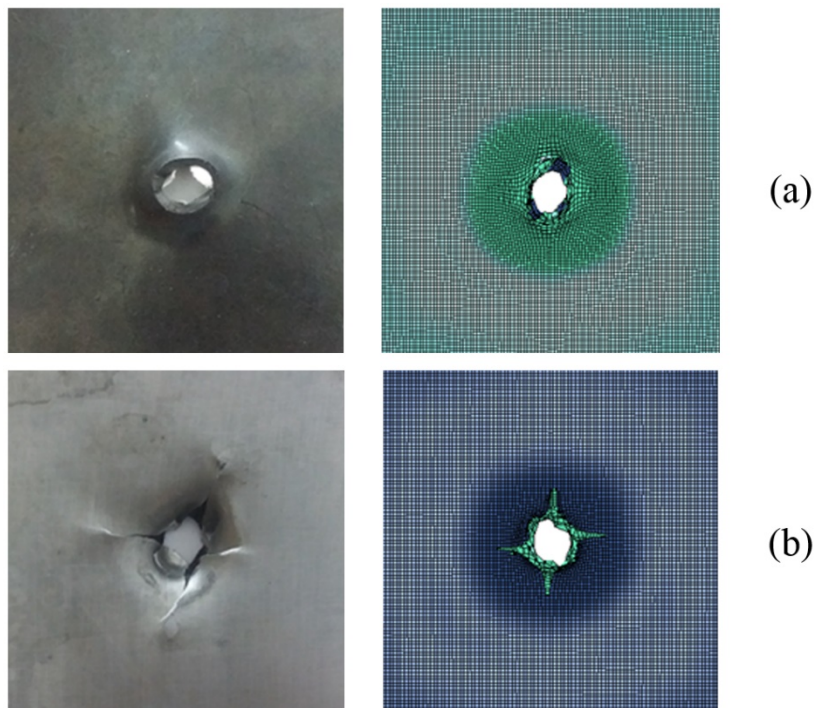


Fig 11 Failure of composite with the rubber on the back face at the impact velocity of 168 m/s obtained Experimentally and numerically (a) Back view (b) Front view

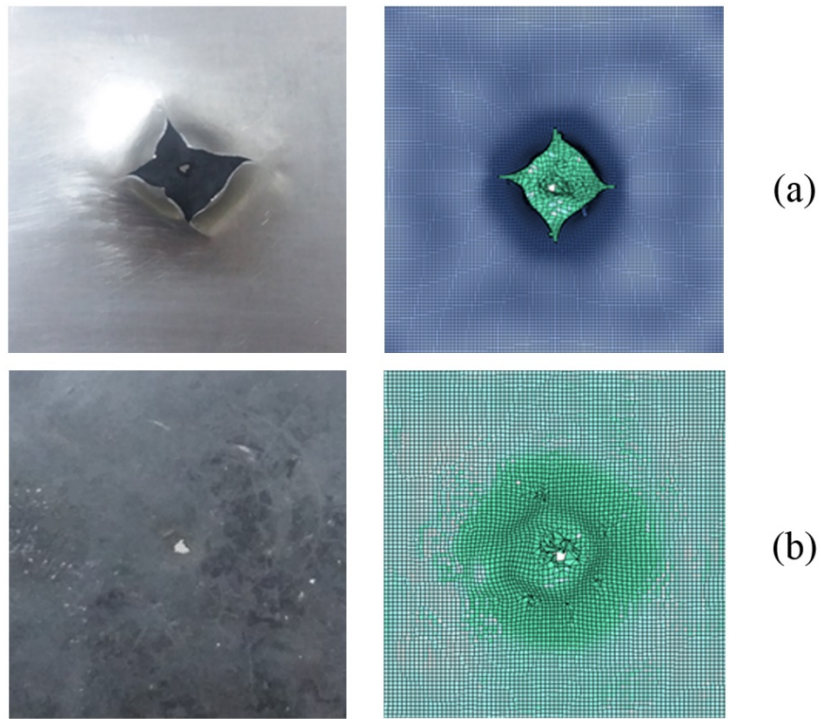


Fig 12 Failure of composite with the rubber on the front face at the impact velocity of 144 m/s obtained Experimentally and numerically (a) Back view (b) Front view

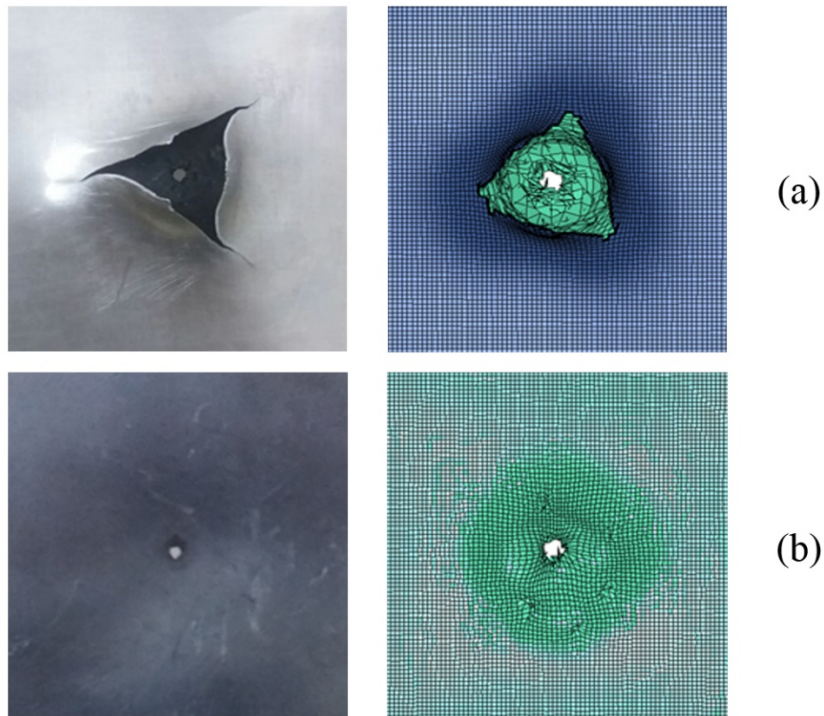


Fig 13 Failure of composite with the rubber on the front face at the impact velocity of 168 m/s obtained Experimentally and numerically (a) Back view (b) Front view

5. Parametric study

A parametric study on the bilayer aluminum-rubber composite plate under impact loading was performed. The main parameters that were investigated are: the relative position of the rubber layer with respect to the loading direction, the effect of different impact velocities, the effect of rubber hardness, the effect of rubber layer thickness, and the strength of rubber-aluminum bonding. The residual velocity of projectile was measured in simulations and the energy absorption of bilayer composite was calculated and considered as a criterion to compare their impact resistance. The projectile used in the finite element models reported in this section has a mass of 9.32 g for all the modeled samples. Also, all the aluminum plate models have thickness of 0.5 mm.

5.1. Effect of relative position

As it is mentioned in the previous section, to study the effect of the relative position of rubber, two configurations of bilayer composite plate were considered. First configuration, the rubber layer was located on the impact receiving side, front face (FF), and second, the rubber panel was located on the back face of impact (BF). In this section numerical simulation was performed in different impact velocities to see the effect of rubber layer position. Also, the ballistic limit (reference velocity) of the composite target was determined. The high hardness (HH) rubber layer was used and the interface shear and normal bonding strength was assumed to be 80 and 50 MPa, respectively. Figure 14 shows the residual velocity of projectile after perforating the bilayer composite versus impact velocity for two BF and FF configurations. Moderate enhancement in ballistic performance in terms of lower residual velocity for bilayer composite plate, which rubber layer located in front face, was observed and compared to the corresponding back face configuration. It was find out that the composite plate by front face

rubber layer configuration shows a better penetration resistance compared to the back face composite plate.

The ballistic limits obtained by numerical analysis for the composite plate with BF and FF configurations are 84.5 and 95 m/s, respectively. While, in Section 4.1, it was observed that the ballistic limit for the single-layer aluminum plate is 50.5 m/s. Comparing the ballistic limit of the bilayer aluminum-rubber composite with the ballistic limit of the aluminum plate shows the rubber layer with high damping properties has a significant effect on the energy absorption of the composite target. Increase in the ballistic limit of composite with the BF and FF configurations is 67.3% and 88.1%, respectively.

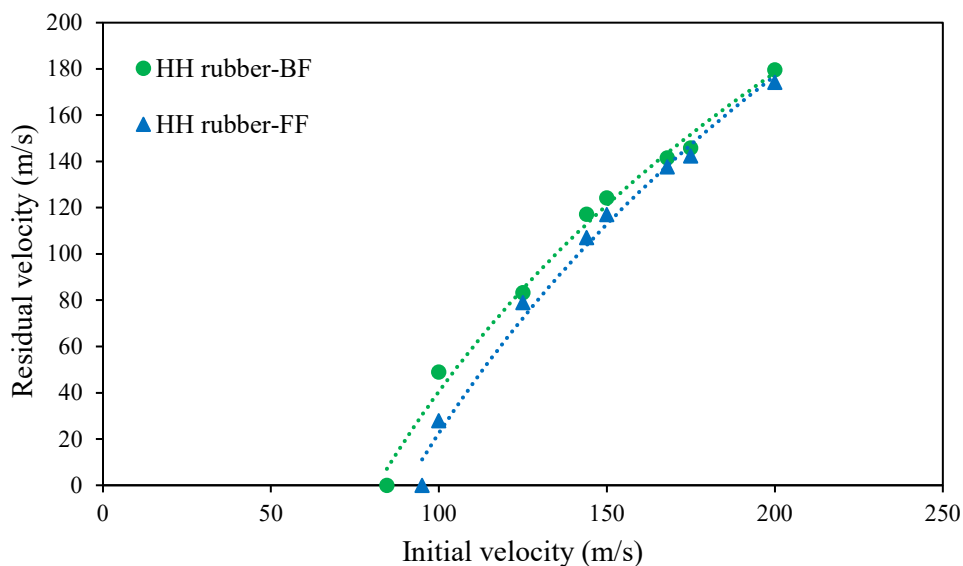


Fig 14 Residual velocities versus initial velocities of Al-HH rubber composite for BF and FF configuration

5.2. Effect of rubber hardness

It is known that in rubber material the formulation of its component has influence on the its mechanical properties and its impact resistance properties. In this section the numerical simulation was performed on the bilayer aluminum-low hardness rubber (LH) composite plate

and compared to the composite plate made by HH rubber. Figs. 15 and 16 show the residual velocity of projectile versus initial velocity after perforation of two type composite with HH and LH rubber layer for BF and FF configuration. The figures show higher ballistic performance in term of lower residual velocity for the composite plate made by HH rubber compared to corresponding LH rubber composite plate. This advantage is applicable for both BF and FF configurations. The higher energy absorption capacity of HH rubber compare to LH rubber can be referred to its stronger molecular chains.

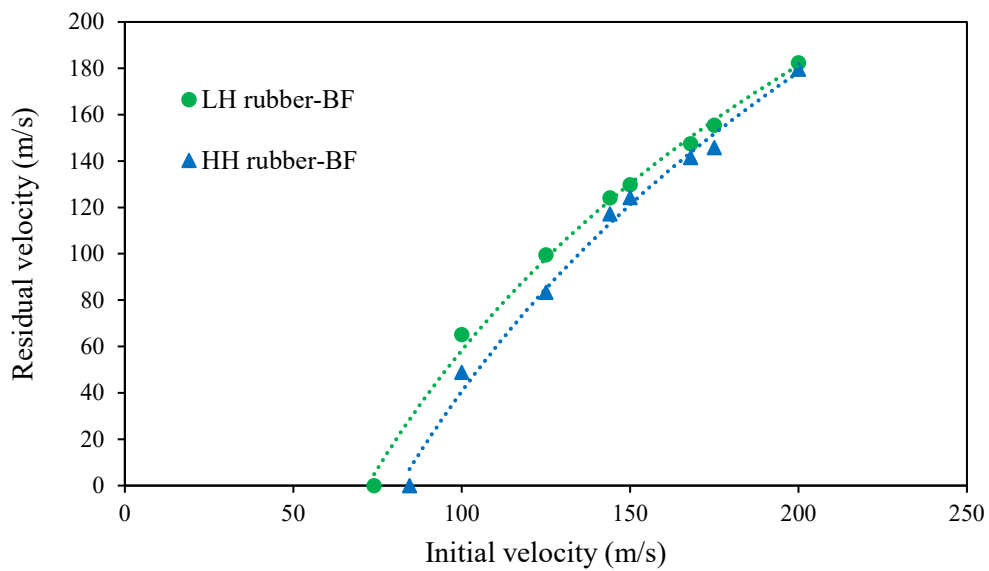


Fig 15 Residual velocities versus initial velocities of Al-rubber composite with LH and HH rubber layer for BF configuration

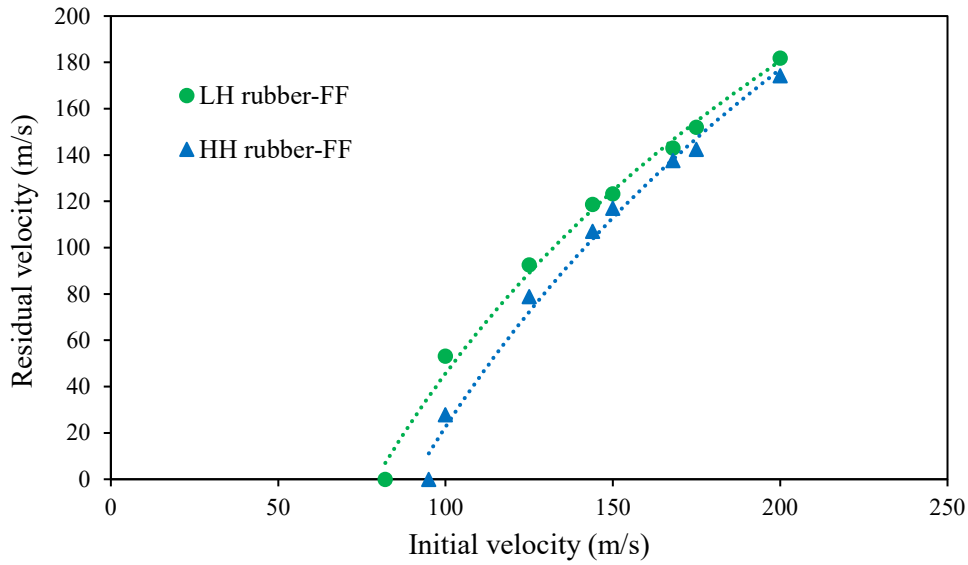


Fig. 16 Residual velocities versus initial velocities of Al-rubber composite with LH and HH rubber layer for FF configuration

Fig. 17 illustrates the projectile velocity histories at impact velocity of 150 m/s on the bilayer composites plate made by LH and HH rubber layers for BF and FF configurations. As it shown in the figure, the specimens perforation and the residual velocities are different. From observations of Figure 17, following points are notable:

(i) The velocity deceleration rate of the projectile impacting the composite target with HH rubber is higher than the LH case, which means the deceleration rate of the composite sample is directly related to the hardness of the rubber.

(ii) The residual velocity of the projectile impacting the aluminum-HH rubber layer is lower than the aluminum-LH rubber composite sample.

(iii) The first level of BF configuration behavior is affected by the aluminum performance causing the intense deceleration of the projectile velocity. After failure of the aluminum plate, the gradient is gentle due to low module and large elongation to failure of the rubber.

(iv) Time duration of penetration is longer for the composites targets with FF configuration compared with the composites targets with BF configuration.

(v) The residual velocity of the projectile impacting on the composite plate with FF configuration is lower compared to BF configuration.

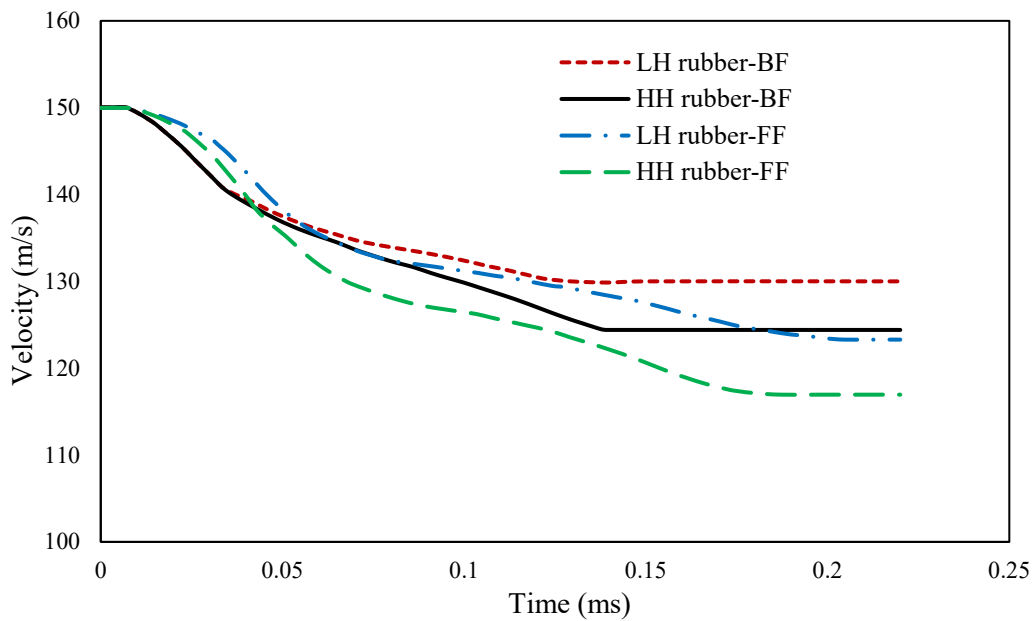


Fig. 17 Comparison of projectile velocity histories at impact velocity of 150 m/s on LH and HH rubber-Al composite for BF and FF configuration

5.3. Effect of rubber layer thickness

A set of simulations is performed to study the effect of the rubber layer thickness on the performance of the bilayer Al-rubber composite target. In these simulations the thicknesses of the rubber layer used for the simulations were 0.5 mm, 1 mm, 1.5, 2 mm, 2.5 mm, and 3 mm, as shown in Table 4. The simulations are performed for both BF and FF configurations. The HH rubber layer was used and the interface shear stress and normal stress at bonding interface was assumed to be 80 MPa and 50 MPa, respectively.

Fig. 18 compares the energy absorption of each composite plates with different rubber layer thickness. The comparison reveals that the increase in the thickness of the rubber layer improves the overall performance of the bilayer plates for both BF and FF configuration. In the case of FF configuration the rubber thickness is more effective, in which increasing the rubber layer thickness, significantly increase the energy absorption of the composite target.

Table 4 Numerical modeling of Al-rubber composite with different rubber thickness

Al thickness (mm)	Rubber thickness (mm)	Al-rubber composite
0.5	0.5	
	1	
	1.5	
	2	
	2.5	
	3	

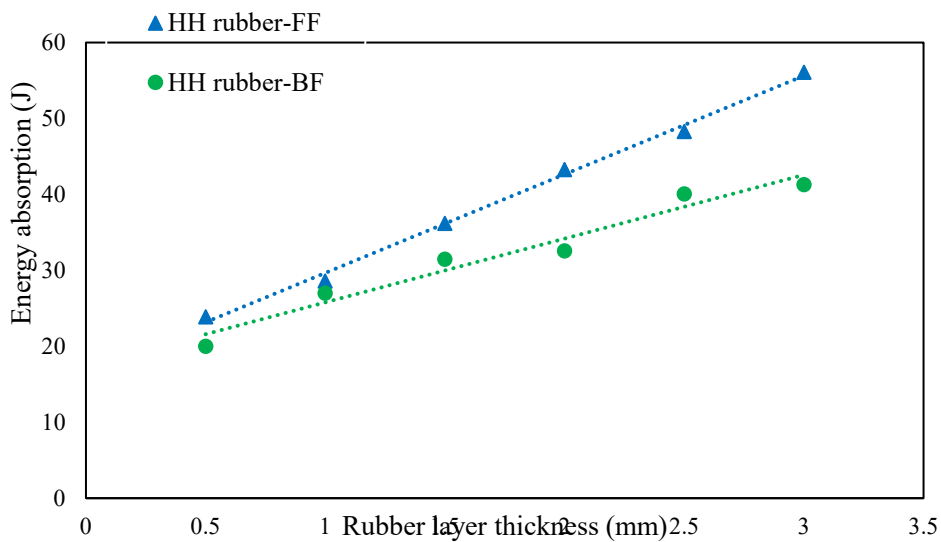


Fig 18 Energy absorption of Al-HH rubber composite with different rubber layer thickness For BF and FF configuration

5.4. Effect of bonding

A simulation was performed to evaluate the effect of the aluminum-rubber interface bonding strength on the performance of the bilayer composite plate. The thickness of aluminum and rubber layer were 0.5 mm and 2 mm, and HH rubber was used in these simulations. The initial velocity of projectile was set to be 144 m/s for each simulation. For all simulation residual velocity was measured and the energy absorption was calculated. The values of the bonding strength used for these simulations are from the low to high bonding values. Six values of interface bonding strength were considered in this study and simulation was performed to evaluate the ballistic performance of each configuration and bonding interface. The bonding values between rubber and aluminum layer were considered to be 0-0 (which means two layer does not have any bonding and are separated with each other), 20S-12N, 40S-24N, 60S-36N, 80S-48N, and Tie (perfect bonding). Fig. 19 shows the energy absorption capacity of the bilayer composite plate with BF and FF configurations with different interface bonding strength. It can be seen that increase bonding has negative effect on ballistic performance of composite for both BF and FF configurations. This parameter specially affects the BF configuration. It is shown that in Bf configuration when there is no bonding, rubber plate can stretch without any limitation and have the best performance. By increasing the interface bonding between the rubber and aluminum plate, the energy absorption of bilayer composite decreases. It can be seen that there is a critical interface bonding point which BF and FF configurations has same performance. BF configuration has the better performance for

interface bonding values less than critical point. On the other hand, by increasing the bonding beyond the critical point, the FF configuration has better performance.

Figs. 20 and 21 show the deformation of bilayer composite for BF and FF configuration, respectively. It can be seen that bonding restricts the rubber deformation and doesn't let the rubber layer to present its stretch and damping properties.

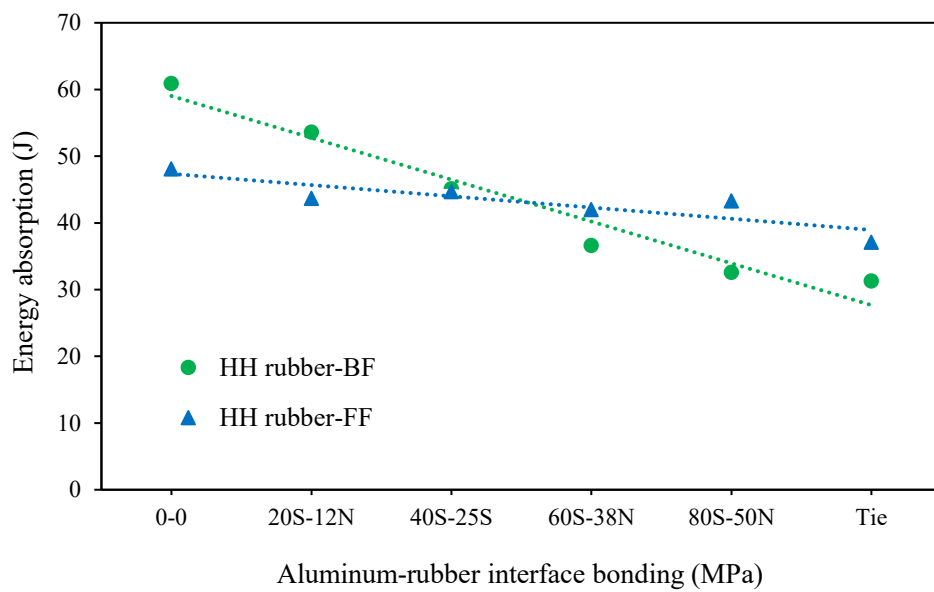


Fig 19 Energy absorption of Al-HH rubber composite with different interface bonding For BF and FF configuration

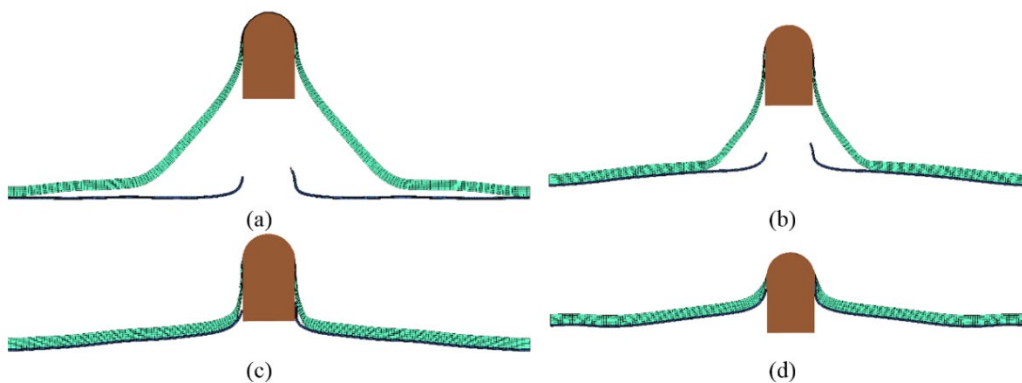


Fig 20 Impact behavior of Al-rubber composite at initial velocity of 144 m/s with different interface bonding for BF configuration

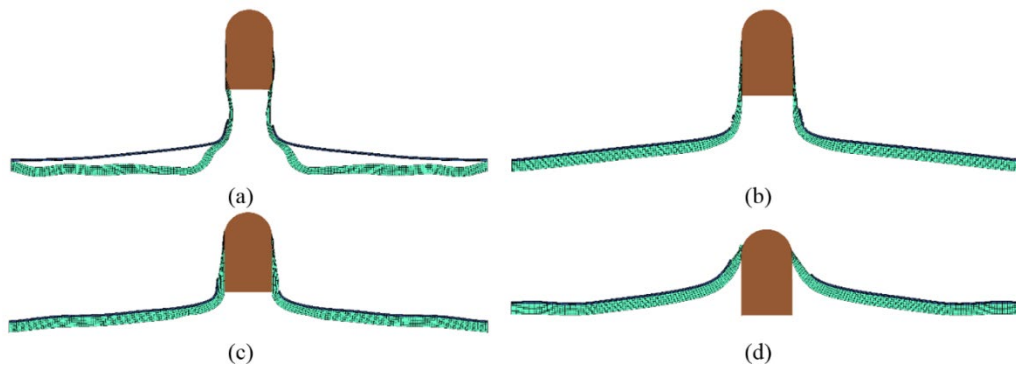


Fig 21 Impact behavior of Al-rubber composite at initial velocity of 144 m/s with different interface bonding for FF configuration

6. Conclusion

In this paper, mechanical behavior of an aluminum-rubber bilayer composite target plate under high velocity impact loading was investigated. A series of experimental tests were conducted using a high velocity gas gun at projectile velocities of 144 m/s and 168 m/s. From the experiments, it was focused on the ballistic performance of composite plate considering the relative position of the rubber layer with respect to the loading direction. It was found that when rubber layer located on the front face of bilayer aluminum-rubber composite, better ballistic performance can be achieved. A numerical simulation in parallel with experimental tests was developed. The simulation was supported using a parametric study on bilayer aluminum-rubber composite. Rubber mechanical properties, as a strain rate dependent material, were obtained by SHPB tests and assigned to the model. A close agreement was found between numerical and experimental results.

Following conclusions can be highlighted from the parametric study:

1- The ballistic limits of bilayer composite with BF and FF configuration were 84.5 and 95 m/s, respectively which shows 67.3% and 88.1% increase compared to the ballistic limit of the monolithic aluminum plate.

2- The ballistic performance of aluminum-rubber composite is highly dependent onto the hardness of rubber. The composite sample with higher hardness rubber can resist more efficiently against the projectile impact.

3- Increase the thickness of the rubber layer improves the overall performance of the bilayer plates for both BF and FF configurations. On the other hand, the FF configuration is more sensitive to the rubber thickness.

4- By increasing the interface bonding between the rubber and aluminum plate, the energy absorption of bilayer composite target decreases. There is a critical threshold for the interface bonding. For the case of BF configuration, the energy absorption would be higher if the bonding values is less than critical point. For the case of FF configuration, by increasing the bonding strength beyond the critical point, the ballistic performance would be higher.

References

- [1] Tiwari G, Iqbal M, Gupta P. Energy absorption characteristics of thin aluminium plate against hemispherical nosed projectile impact. *Thin-Walled Structures*. 2018;126:246-57.
- [2] Rosenberg Z, Kositski R, Dekel E. On the perforation of aluminum plates by 7.62 mm APM2 projectiles. *International Journal of Impact Engineering*. 2016;97:79-86.
- [3] Iqbal M, Khan S, Ansari R, Gupta N. Experimental and numerical studies of double-nosed projectile impact on aluminum plates. *International Journal of Impact Engineering*. 2013;54:232-45.
- [4] Rodriguez-Millan M, Garcia-Gonzalez D, Rusinek A, Abed F, Arias A. Perforation mechanics of 2024 aluminium protective plates subjected to impact by different nose shapes of projectiles. *Thin-Walled Structures*. 2018;123:1-10.
- [5] Amini M, Simon J, Nemat-Nasser S. Numerical modeling of effect of polyurea on response of steel plates to impulsive loads in direct pressure-pulse experiments. *Mechanics of Materials*. 2010;42:615-27.
- [6] Amini M, Isaacs J, Nemat-Nasser S. Investigation of effect of polyurea on response of steel plates to impulsive loads in direct pressure-pulse experiments. *Mechanics of Materials*. 2010;42:628-39.

- [7] Roland C, Fragiadakis D, Gamache R. Elastomer–steel laminate armor. *Composite Structures*. 2010;92:1059-64.
- [8] Roland C, Fragiadakis D, Gamache R, Casalini R. Factors influencing the ballistic impact resistance of elastomer-coated metal substrates. *Philosophical Magazine*. 2013;93:468-77.
- [9] Grujicic M, Pandurangan B, He T, Cheeseman B, Yen C-F, Randow C. Computational investigation of impact energy absorption capability of polyurea coatings via deformation-induced glass transition. *Materials Science and Engineering: A*. 2010;527:7741-51.
- [10] Yang H, Yao X-F, Wang S, Ke Y-C, Huang S-H, Liu Y-H. Analysis and Inversion of Contact Stress for the Finite Thickness Neo-Hookean Layer. *Journal of Applied Mechanics*. 2018;85:101008.
- [11] Pouriayevali H, Guo Y, Shim V. A visco-hyperelastic constitutive description of elastomer behaviour at high strain rates. *Procedia Engineering*. 2011;10:2274-9.
- [12] Yang H, Yao X, Zheng Z, Gong L, Yuan L, Yuan Y, et al. Highly sensitive and stretchable graphene-silicone rubber composites for strain sensing. *Composites Science and Technology*. 2018;167:371-8.
- [13] Hassim N, Ahmad MR, Ahmad WYW, Samsuri A, Yahya MHM. Puncture resistance of natural rubber latex unidirectional coated fabrics. *Journal of Industrial Textiles*. 2012;42:118-31.
- [14] Dong Y, Ke Y, Zheng Z, Yang H, Yao X. Effect of stress relaxation on sealing performance of the fabric rubber seal. *Composites Science and Technology*. 2017;151:291-301.
- [15] Yang H, Yao X-F, Ke Y-C, Ma Y-j, Liu Y-H. Constitutive behaviors and mechanical characterizations of fabric reinforced rubber composites. *Composite Structures*. 2016;152:117-23.
- [16] Yang H, Yao X-F, Yan H, Yuan Y-n, Dong Y-F, Liu Y-H. Anisotropic hyper-viscoelastic behaviors of fabric reinforced rubber composites. *Composite Structures*. 2018;187:116-21.
- [17] Bhattacharya M, Bhowmick AK. Synergy in carbon black-filled natural rubber nanocomposites. Part I: Mechanical, dynamic mechanical properties, and morphology. *Journal of materials science*. 2010;45:6126-38.
- [18] Cai HH, Li SD, Tian GR, Wang HB, Wang JH. Reinforcement of natural rubber latex film by ultrafine calcium carbonate. *Journal of applied polymer science*. 2003;87:982-5.
- [19] Manroshan S, Baharin A. Effect of nanosized calcium carbonate on the mechanical properties of latex films. *Journal of applied polymer science*. 2005;96:1550-6.
- [20] Li X, Li Z, Xia Y. Test and calculation of the carbon black reinforcement effect on the hyper-elastic properties of tire rubbers. *Rubber Chemistry and Technology*. 2015;88:98-116.
- [21] Yang L, Shim V, Lim C. A visco-hyperelastic approach to modelling the constitutive behaviour of rubber. *International Journal of Impact Engineering*. 2000;24:545-60.
- [22] Bai Y, Liu C, Huang G, Li W, Feng S. A Hyper-Viscoelastic Constitutive Model for Polyurea under Uniaxial Compressive Loading. *Polymers*. 2016;8:133.
- [23] Manual L-DKUs, Volume I. Version 971. Livermore Software Technology Corporation. 2007;7374:354.
- [24] Spranghers K, Kakogiannis D, Ndambi J, Lecompte D, Sol H. Deformation measurements of blast loaded plates using digital image correlation and high-speed photography. *EPJ Web of Conferences: EDP Sciences*; 2010. p. 12006.
- [25] Ghalami-Choobar M, Sadighi M. Investigation of high velocity impact of cylindrical projectile on sandwich panels with fiber–metal laminates skins and polyurethane core. *Aerospace Science and Technology*. 2014;32:142-52.

- [26] Khodadadi A, Liaghat G, Ahmadi H, Bahramian AR, Anani Y, Razmkhah O, et al. Numerical and experimental study of impact on hyperelastic rubber panels. *Iranian Polymer Journal*. 2018:1-10.